Effect of Coadsorbed Oxygen on the Chemistry of Ammonia over Ni(110) Single-Crystal Surfaces

Hansheng Guo, Demetrius Chrysostomou, Jefferson Flowers, and Francisco Zaera*

Department of Chemistry, University of California, Riverside, Riverside, California 92521

Received: July 15, 2002; In Final Form: October 23, 2002

The surface chemistry of ammonia coadsorbed with atomic oxygen on Ni(110) single-crystal surfaces was studied by temperature-programmed desorption (TPD) and X-ray photoelectron spectroscopy (XPS). At intermediate oxygen coverages, direct ammonia adsorption on nickel sites is suppressed, but a new high-temperature reaction regime is generated. Desorption of ammonia from rehydrogenation of NH_x surface fragments (identified by XPS) takes place around 400 K, concurrently with the production of water and molecular hydrogen. Experiments with deuterium labeling indicated extensive isotope scrambling and hydrogen transfer from nitrogen- to oxygen-containing surface intermediates. The optimum yields seen for this 400 K state at intermediate oxygen coverages strongly suggest the direct interaction of the adsorbed ammonia with oxygen atoms at the end of the −Ni−O− rows that form upon reconstruction of the surface. Hydrogen transfer between ammonia and oxygen appears to take place directly via hydrogen bonding, and to be reversible but biased toward water formation. An equilibrium is reached between the produced water and the reacting surface oxygen and hydrogen.

1. Introduction

It is well known that oxygen chemisorbed on metal surfaces can facilitate the activation of a number of adsorbates such as water,[1] hydrogen sulfide,[2] ammonia,[3] organic acids,[4,5] and other hydrocarbons.[6,7] Oxygen incorporation into metal−carbon bonds has also been reported in surface-science studies[8−11] and is a recognized pathway to hydrocarbon oxidation.[12] However, different oxygen surface species, such as dioxygen,[13] superoxides[14] and peroxides,[15] are believed to lead to different chemical behavior. Atomic oxygen is perhaps the most common intermediate involved in the surface chemistry of hydrocarbons in catalysis, but even there, different adsorption states lead to different reactivity. For instance, the reaction of alkanes with adsorbed oxygen atoms is thought to favor the formation of carbon dioxide, whereas lattice oxygen seems to be required for the formation of alcohols, aldehydes, and other oxygenated hydrocarbons.[16] Hydroxyl groups are also crucial participants in many surface and catalytic processes.[11,17−21]

Ammonia is an ideal probe to characterize the nature of the oxygen species present on catalytic surfaces. In fact, changes in adsorption geometry and surface chemistry induced by coadsorbed oxygen have already been reported on many metal surfaces.[22−27] This chemistry between ammonia and oxygen may often be understood in terms of fundamental principles such as electronegativity and acid−base properties, but may be complicated further on open surfaces because of oxygen-induced surface reconstructions.[28,29] Of particular importance to this report is the establishment of the −Ni−O− rows that grow in the [001] direction of (110) planes of nickel,[28] silver,[30] and copper[31] surfaces upon oxygen uptake. Those structures offer a unique opportunity for the study of the chemical behavior of different oxygen species, particularly that of the oxygen atoms at the end of the reconstructed rows. Surface-science studies of ammonia on oxygen-predosed surfaces is likely to provide new insights into the nature of oxidation catalysts, and to help in the understanding of catalytic processes such as ammonia synthesis[32,33] and hydrocarbon ammoxidation.[34]

Below, the main results from our temperature-programmed desorption (TPD) and X-ray photoelectron spectroscopy (XPS) studies on the chemistry of ammonia and atomic oxygen coadsorbed on Ni(110) single-crystal surfaces are analyzed. This work corroborates a previous report[23] of a new chemical state around 400 K associated with hydrogen transfer between nitrogen- and oxygen-containing adsorbates. The new chemistry is explained in terms of hydrogen bonding between adjacent reactants directly bonded to nickel atoms. In addition, given that the yield maxima for water and ammonia desorption at 400 K are seen at intermediate oxygen coverages, it is proposed that the oxygen at the end of the reconstructed −Ni−O− rows are the responsible for the ammonia to water conversion. A preference toward water formation is manifested by extensive isotope scrambling in experiments with ND_3 and by the establishment of an equilibrium between H_2O and adsorbed oxygen and hydrogen on the surface, and is easily understood in terms of the higher electronegativity of oxygen compared to nitrogen atoms. The role of hydroxyl surface groups in the surface chemistry of ammonia on nickel will be reported separately.[35]

2. Experimental Section

All experiments were carried out in a turbomolecular-pumped ultrahigh vacuum (UHV) chamber with a base pressure below 1×10^{-10} Torr. This chamber is equipped with a quadrupole mass spectrometer for gas analysis and temperature-programmed desorption (TPD), a 100 mm concentric hemispherical energy analyzer and a twin anode X-ray gun for X-ray photoelectron spectroscopy (XPS), a rasterable ion gun for sample sputtering and ion scattering experiments, and four-grid spherical retarding field optics for low-energy electron diffraction (LEED). The

* Corresponding author. E-mail: francisco.zaera@ucr.edu.

10.1021/jp026530u CCC: $25.00
Published on Web 12/18/2002

mass spectrometer was retrofitted with an extendible nose cone with a 5 mm diameter aperture placed within 1 mm of the single crystal for the selective detection of molecules desorbing from its front face during the TPD experiments, and it was interfaced to a personal computer capable of monitoring the time evolution of up to 15 different masses in a single TPD run. The XPS data were acquired by using an Al anode, and by setting the electron energy analyzer to a fixed pass energy of 50 eV. XPS data acquisition was also performed via an interfaced personal computer, by averaging several scans to increase the signal-to-noise level of the spectra. The details of this experimental setup have been reported elsewhere.[36,37]

The Ni(110) crystal was cut and polished on both sides using standard procedures, and heated resistively via two tantalum wires spot-welded to its edge, which also held the sample mechanically in place. Cooling the crystal to 90 K was done by immersing the heating leads, coupled to the crystal via UHV electrical feedthroughs, into a vertical liquid nitrogen reservoir. Linear heating rates of 5 K/s were used in all the TPD experiments, as generated by using a homemade ramping power supply. A chromel/alumel thermocouple was spot-welded to the edge of the crystal for temperature monitoring. The sample was biased with −100 V in the TPD experiments to minimize any electron-induced damage of the adsorbates.[38,39]

The crystal surface was cleaned under vacuum by cycles of argon ion bombardment and annealing at 900 K, as reported before.[36] Surface cleanliness was checked by both XPS and CO TPD experiments. All gases were purchased from Matheson and used as supplied. H_2 and nondeuterated ammonia (NH_3) were better than 99.99% pure, but the maximum isotope purity of the ND_3 was found independently by NMR to be only about 60%, and measured at about 50% in situ with our mass spectrometer (because of the additional exchange with background H_2 in the ionization region). Exposures of the Ni(110) surface to the different gases were performed by backfilling the vacuum chamber using leak valves, and were measured in langmuirs (1 langmuir $= 1 \times 10^{-6}$ Torr/s), uncorrected for ion gauge sensitivities. The TPD signals are reported in arbitrary units but are referred to a common scale provided by the bar included in most figures.

3. Results

3.1. Temperature Programmed Desorption. The chemistry of ammonia coadsorbed with atomic oxygen on Ni(110) surfaces was first explored by temperature-programmed desorption (TPD). For this, the clean nickel crystal was first exposed to varying amounts of dioxygen gas at either 300 or 400 K to deposit the desired coverage of atomic oxygen on the surface, taking advantage of the fact that O_2 adsorption is dissociative in that temperature range,[40,41] and then cooled to liquid nitrogen temperatures, about 100 K, and dosed with ammonia. Figure 1 displays the series of TPD spectra obtained for 1.5 langmuir exposures to ammonia as a function of oxygen predose at 300 K. The three panels in that figure correspond to the sequences for hydrogen (a, left, 2 amu), ammonia (b, center, 17 amu), and water (c, right, 18 amu) desorption; no other desorbing products were ever observed in these experiments. The 17 amu signal was corrected for the contribution from cracking of water in the mass spectrometer ionizer (about 20% of the 18 amu intensity), even though this correction proved in most cases negligible.

Hydrogen desorption from decomposition of ammonia on clean Ni(110) occurs in two stages peaking at about 348 and 405 K, as already reported in the past.[39,42] These two so-called

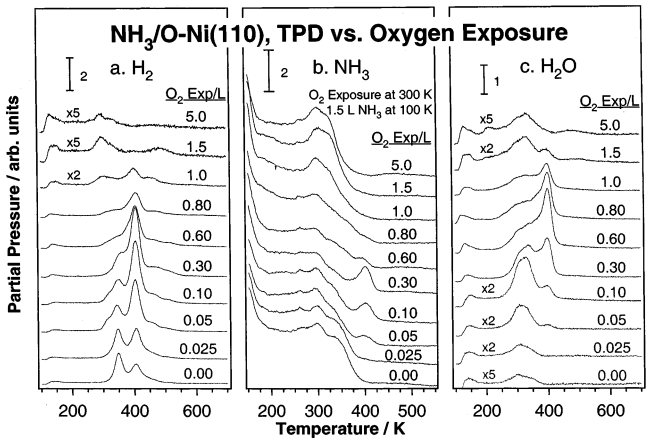

Figure 1. Temperature-programmed desorption (TPD) traces for hydrogen (2 amu, a, left), ammonia (17 amu, b, center), and water (18 amu, c, right) from ammonia adsorbed at 100 K on Ni(110) single-crystal surfaces preexposed with various amounts of oxygen at 300 K. A constant heating rate of 5 K/s was used in all the experiments, and the crystal was biased with −100 V to minimize any possible damage induced by stray electrons. Perhaps the most interesting observation from the data in this figure is the appearance of a new chemical state around 400 K at intermediate oxygen coverages.

β and γ peaks display comparable intensities on clean Ni(110). As the surface is preexposed to increasing amounts of oxygen, however, desorption from the first state becomes reduced at the expense of the second, until appearing only as a shoulder by 0.30 langmuir O_2. In fact, the total hydrogen desorption yield increases substantially up to that 0.30 langmuir O_2 mark, after which it decreases again. A third TPD state about 470 K also develops above 0.050 langmuir O_2 doses. The extent of ammonia decomposition then decreases at the high end of the oxygen exposures, as a film of nickel oxide grows on the surface.[41] After oxygen preexposures in excess of 1.0 langmuir, only a residual amount of hydrogen desorption is observed, in two new states around 300 and 490 K.

The desorption of ammonia from these oxygen-treated Ni(110) surfaces is quite complex, but can basically be divided into three regions, namely: (1) the α state between 250 and 350 K, associated with direct chemisorption to the metal centers via lone-pair electron donation; (2) the β state, centered about 160 K, due to chemisorption on a second layer via hydrogen bonding to the first; and (3) condensed ammonia below 120 K.[39] On the clean surface, the α region shows a complex structure in the TPD traces, with at least three states filling in sequentially with increasing ammonia exposure.[39] However, that fine structure is smoothed as oxygen is predeposited on the surface while the total intensity of the TPD peaks decreases, perhaps because of the blocking of nickel adsorption sites by the oxygen atoms. In addition, a new high temperature state around 400 K appears by 0.050 langmuir O_2, reaches a maximum in intensity about 0.30 langmuir O_2, and disappears again above 1.0 langmuir O_2. This new desorption feature is indicative of new oxygen-induced chemistry, and will be the focus of much of our discussion.

Finally, water production from ammonia adsorbed on clean Ni(110) is almost negligible. No water is expected to be produced in this case, but a small and broad feature is seen between 250 and 380 K, probably because of H_2O adsorption from the background. As oxygen is preadsorbed on the surface, on the other hand, significant water desorbs in the TPD experiments. After a 0.050 langmuir O_2 preexposure, the broad feature around 315 K grows in intensity, and a second feature appears about 395 K. Increasing oxygen predoses lead to a

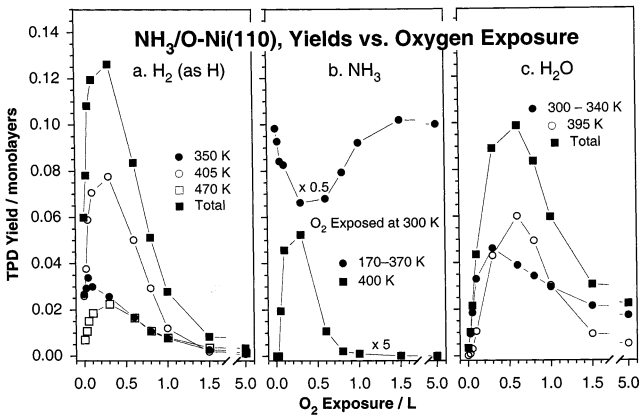

Figure 2. Desorption yields for hydrogen (a, left), ammonia (b, center), and water (c, right) from thermal activation of ammonia coadsorbed with oxygen on Ni(110), calculated after appropriate calibrations from the TPD data reported in Figure 1. The partial yields seen for each of the identifiable desorption states are reported together with the total extent of the desorption for all three products. Again, the new 400 K state that is generated at intermediate oxygen coverages is evident in all three panels. Notice also that water production at 395 K is maximized at oxygen coverages slightly higher than those required for ammonia and hydrogen production (at 400 and 405 K, respectively).

significant increase in water yield, in both states at first, and preferentially in the high-temperature state above 0.10 langmuir O_2. A maximum in TPD peak intensities is reached for 0.60 langmuir O_2, and a monotonic decrease in the population of both states follows, until only a small amount of low-temperature desorption remains (above 1.0 langmuir O_2). The two desorption states, previously denoted as A and B, have also been reported in studies with water on clean and oxygen-predosed Ni(110) surfaces, and correspond to molecular desorption and hydroxyl group disproportionation, respectively.[43,44]

Integration of the TPD traces in Figure 1, after appropriate calibration,[39] provides information on the desorption yields. The results are displayed in Figure 2. Hydrogen desorption from total ammonia decomposition increases initially with oxygen predose, from about 0.030 monolayer H_2 on the clean surface, to a maximum of ~0.066 monolayer for a 0.30 langmuir O_2 predose, and then decreases again until reaching a value close to zero on the NiO film (an O_2 predose of >5 langmuirs). The low-temperature (350 K) peak, which may include some adsorption from the background, decreases almost linearly with oxygen dose, perhaps because of site blocking by the atomic oxygen, but the other two features follow trends similar to that of the total yield. The overall molecular desorption of ammonia first decreases, from 0.20 monolayer on the clean nickel to about 0.13 monolayer after a 0.30 langmuir O_2 predose, but then recovers its original value as an oxide film grows on the surface. Interestingly, though, the new high-temperature feature about 400 K appears, goes through a maximum, and disappears again in roughly the same oxygen predose region where the dip in total molecular desorption yield is observed. In terms of water desorption, the trend of the 395 K peak intensity, as well as that of the total yield, follows closely that of the total hydrogen desorption. The low-temperature (300−340 K) desorption, however, peaks at an earlier oxygen predose, and decreases slowly afterward. Finally, it is worth noting that the high-temperature ammonia peak starts to appear and reaches its yield maximum at lower oxygen predoses than either the water B peak or the hydrogen γ feature. The hydrogen, ammonia, and water yields for the high temperature (~400 K) TPD state are reported as a function of oxygen predose in Table 1.

Additional TPD studies were performed to characterize the uptake of ammonia on Ni(110) surfaces with different oxygen precoverages. Figure 3 displays the TPD yield trends observed as a function of ammonia dose for the case of a 0.50 langmuir O_2 predose. The amounts of hydrogen desorption in both the 350 and 405 K peaks grow approximately linearly with ammonia dose (at least up to about 1.0 langmuir), suggesting that total decomposition of a significant and fixed fraction of that ammonia takes place at all oxygen coverages. The same is true for the total yield of water, except that the peak shapes do change significantly with ammonia coverage: the 395 K fills in preferentially, almost exclusively, up to 0.40 langmuir NH_3, but then levels off as the low-temperature peak develops. Molecular ammonia is not detected at all at low coverages; only after a 0.40 langmuir NH_3 dose does a small amount desorb-molecularly about 400 K. This high-temperature state then gets filled in an approximately linear fashion with an ammonia dose, the same as the α (250−350 K) region above 0.60 langmuir NH_3. Ammonia condensation starts at 1.5 langmuirs.

The total ammonia uptake versus exposure can be calculated from the data in Figure 3 after taking into account the corresponding stoichiometries of the various products, and the slope of those uptake curves at the low exposure end can then be used to estimate the initial sticking coefficients, S_o. The S_o values obtained this way for different oxygen precoverages are summarized in the inset of Figure 3 (raw data not shown). There is a significant drop in the initial sticking coefficient of ammonia as oxygen is predeposited on the Ni(110) surface, from about 0.46 on the clean substrate to 0.22 after a 0.50 langmuir O_2 predose, and a subsequent slight increase at higher oxygen coverages. This trend roughly matches that seen for the ammonia molecular desorption yields.

The surface atomic nitrogen resulting from ammonia total dehydrogenation recombines around 800 K to desorb as molecular nitrogen, N_2. TPD data for this desorption is presented in Figure 4 as a function of oxygen predose. Despite its weak intensity, the 14 amu signal was chosen to differentiate between N_2 and CO production (the 28 amu traces yielded similar results, but showed some interferences from CO desorption from the sample holder). There is a clear increase in nitrogen yield at intermediate oxygen surface concentrations. After calibration using both XPS (see below) and previous TPD data from ammonia on clean Ni(110),[39] desorption yields were calculated; the data are shown in the inset of Figure 4, and also reported in Table 1. The maximum in ammonia decomposition is seen around 0.25 langmuir O_2 preexposures, roughly the same range where the high temperature (~400 K) chemistry is observed.

3.2. X-ray Photoelectron Spectroscopy. The nature of the adsorbed species produced by thermal activation of ammonia coadsorbed with atomic oxygen on Ni(110) single-crystal surfaces was probed by using X-ray photoelectron spectroscopy (XPS). Figure 5 displays the sequence of N 1s (left) and O 1s (right) XPS traces obtained as a function of annealing temperature from 2.0 langmuirs of ammonia adsorbed on a Ni(110) surface predosed with 0.10 langmuir of oxygen at 400 K. Gaussian curves (solid lines) were fitted to the raw data (dots) to facilitate the analysis. The peak fit was performed collectively by fixing most of the peak positions and peak widths to minimize the number of fitting parameters. Initial peak positions were chosen on the basis of reported values for adsorbed ammonia and atomic nitrogen[3] and for atomic oxygen and hydroxide groups,[45] but then left to vary during the fit except that the same values were forced for all the spectra. Control experiments were carried out to make sure that neither the X-ray

TABLE 1: Surface Concentrations and Calculated Reaction Quotients (*Q*) for the High-Temperature (~400 K) Ammonia Chemistry on Oxygen-Predosed Ni(110) Single-Crystal Surfaces

O_2 exp/L	405 K H_2/monolayer	400 K NH_3/monolayer	395 K H_2O/monolayer	Θ_N, 370 K monolayer	Θ_O, 370 K monolayer	$Q(2)^a$	$Q(3) \times 1000$/ monolayer^3 [a]	$Q(5) \times$ monolayer[a]
0.000	0.0130		0.0001	0.023	0.000			
0.025	0.0189		0.0009	0.036	0.006			8.1
0.050	0.0295	0.0039	0.0030	0.050	0.011	3.0	4.3	8.8
0.100	0.0353	0.0091	0.0105	0.078	0.027	4.4	3.2	11.1
0.300	0.0388	0.0105	0.0432	0.130	0.134	5.2	9.0	8.3
0.600	0.0251	0.0022	0.0602	0.052	0.321	3.8	9.2	7.5
0.800	0.0147	0.0004	0.0495	0.007	0.446	0.4	0.9	7.6
1.000	0.0061	0.0002	0.0304	0.007	0.570	0.2	0.2	8.8
1.500	0.0010	0.0000	0.0093		0.879			10.9
					Average	2.8	4.5	8.9
					Std. Dev.	2.1	3.9	1.4

[a] The reaction quotients refer to the following reactions: (2) $2NH_3 + 3O(ads) = 3H_2O + 2N(ads)$; (3) $2NH_3 = 2N(ads) + 3H_2$; (5) $H_2 + O(ads) = H_2O$.

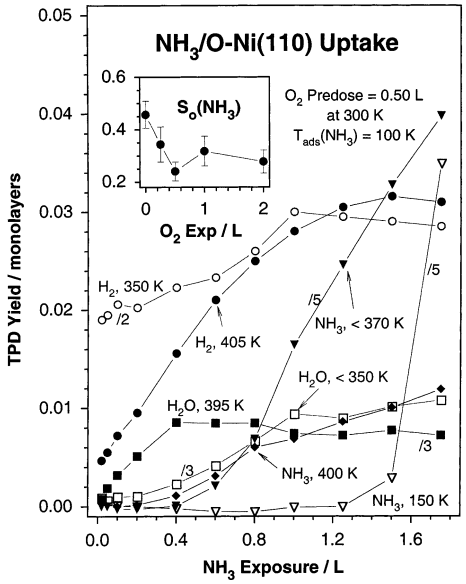

Figure 3. TPD yields for hydrogen, ammonia, and water as a function of ammonia dose for the case of a Ni(110) surface preexposed to 0.50 langmuir O_2 at 300 K. The high-temperature hydrogen (405 K) and water (395 K) peaks grow first, and the 400 K ammonia state appears before the lower temperature NH_3 features. By adding all yields, using appropriate stoichiometric considerations, uptake curves (total ammonia coverage versus exposure) were estimated, and from the initial slope in those, initial sticking coefficients were extracted. The results are reported in the inset as a function of oxygen predose. Notice the dip around 0.5 langmuir O_2 preexposures, approximately the same regime where the 400 K reactions are seen.

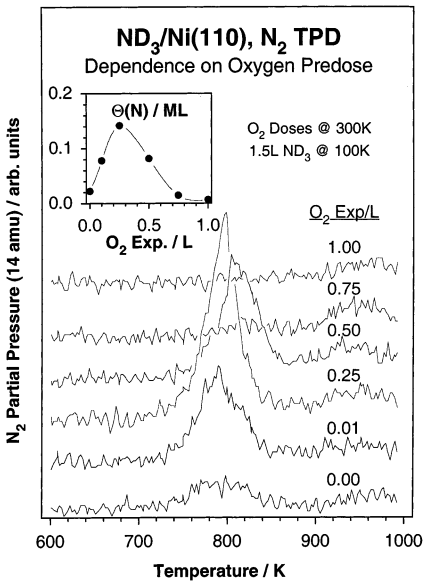

Figure 4. N_2 (14 amu) TPD traces from Ni(110) surfaces dosed sequentially with various amounts of oxygen (at 300 K) and 1.5 langmuirs of deuterated ammonia (at 100 K). The data represent the recombination of the atomic surface nitrogen produced by ammonia total dehydrogenation, and is therefore a good measure of the extent of ND_3 decomposition. The measured nitrogen yields are reported as a function of oxygen predose in the inset. The dependence of the yields for ammonia decomposition on oxygen coverage show an excellent correlation with that for the 400 K desorption state.

radiation nor the resulting photoelectrons induced any spurious chemistry in this system. Adsorbed ammonia is known to be quite sensitive to electron irradiation,[38] but no damage of the ammonia monolayers was seen under our experimental conditions.

The N 1s XPS data in Figure 5 could be separated into three contributions. At 100 K, only one large peak is seen around 399.5 eV, associated with molecular ammonia.[3] After annealing above 200 K, molecular desorption from both multilayers and the second (β) layer are complete, and only monolayer species survive on the surface. The N 1s XPS spectrum for that temperature shows a main feature at 399.7 eV, and a smaller second peak about 397.2 eV. The shift toward higher binding energies seen for the signal from the molecular species (the main peak) results from the elimination of the ammonia clusters associated with the β-NH_3 state.[46] The high-energy signal is here assigned to NH_2 and/or NH adsorbed species. Our binding energy value for those species is significantly lower than that previously reported,[3] but the assignment is consistent with the identification of dehydrogenated nitrogen-containing species by vibrational spectroscopy[25,42] and electron-stimulated desorption.[23] Annealing to higher temperatures leads to an increase in the intensity of the 397.2 eV signal at the expense of that around 399.7 eV, until the former becomes dominant above 300 K. By 350 K a third peak due to chemisorbed atomic nitrogen grows in about 396.6 eV, and by 420 K most of the XPS intensity is centered around that value. Recall that, according to the TPD data, all the hydrogenation−dehydrogenation chemistry is over by 400 K.

The O 1s XPS data presented in the right panel of Figure 5 indicate the presence of at least two oxygen-containing species on the surface. Indeed, the peak at 530.6 eV, which dominates at low temperatures, can be easily assigned to adsorbed atomic oxygen.[41,47,48] On the other hand, the smaller second feature that is always seen about 532.4 eV most likely corresponds to hydroxyl surface groups.[49−51] No adsorbed water was ever

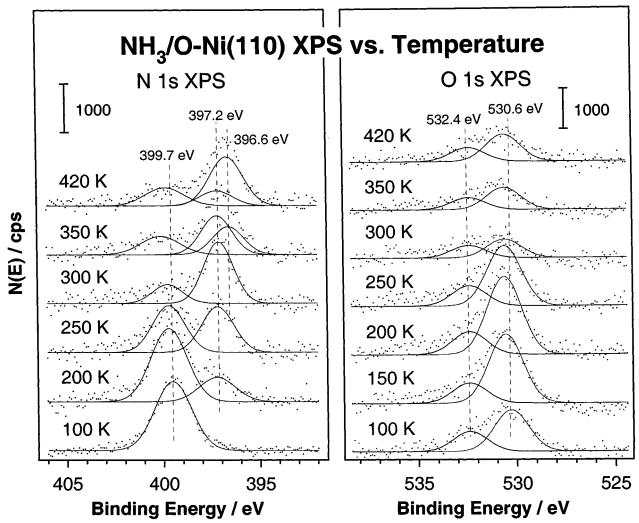

Figure 5. N 1s (left) and O 1s (right) X-ray photoelectron spectroscopy (XPS) data for 2.0 langmuirs of ammonia adsorbed at 100 K on a Ni(110) crystal previously treated with 0.10 langmuir O_2 at 400 K. The nitrogen XPS traces could be fitted to three Gaussian peaks centered about 399.7, 397.2, and 396.6 eV, assigned here to chemisorbed ammonia, NH and/or NH_2 surface species, and adsorbed atomic nitrogen, respectively. The O 1s data display two features around 530.6 and 532.4 eV, associated with atomic oxygen and surface hydroxyl groups, respectively.

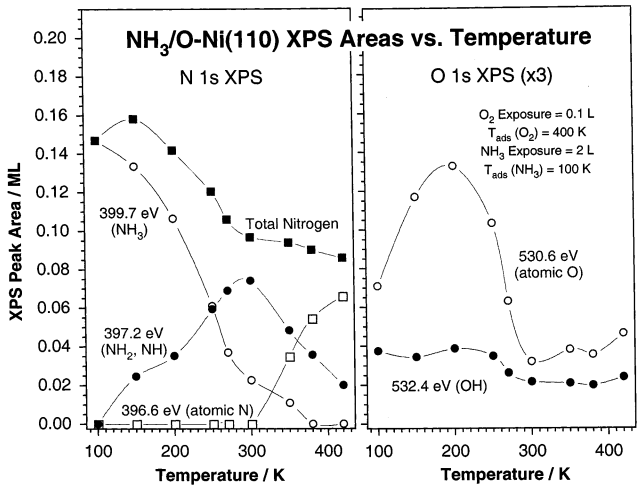

Figure 6. Surface concentrations for the different nitrogen- (left) and oxygen-containing (right) surface species identified in the XPS experiments reported in Figure 5. The signals were calibrated by using reference systems (see text), and are reported in monolayers. Significant ammonia and water desorption is manifested by the noticeable drops in total surface concentrations of N- and O-containing species between approximately 200 and 300 K. In addition, the N 1s XPS peak associated with partially dehydrogenated (NH, NH_2) ammonia grows progressively between 100 and 300 K but then decreases again in intensity at higher temperatures.

detected in these experiments, most likely because H_2O desorbs immediately after being produced. A significant reduction in the population of oxygen species is seen between 200 and 300 K, the range where water desorption is detected in the TPD experiments.

A quantitative analysis of the XPS signal intensities was performed to follow the concentrations of the different adsorbed species as a function of annealing temperature. The results are shown in Figure 6. The signals were calibrated to units of monolayers by using reference systems, the c(4×2) ammonia overlayer known to form on the clean surface in the case of the N 1s XPS,[39] and the (2×1) O/Ni(110) structure for the O 1s XPS spectra.[36]

A clear decrease in the concentration of all nitrogen-containing species of a bit over 0.05 monolayer (about 40% of the total) takes place between 150 and 300 K, in accordance with the different desorption states seen in the ammonia TPD spectra in Figure 1. There is also a progressive conversion of adsorbed ammonia to NH_x ($x = 1$ or 2) species between 100 and 300 K, indicative of the ability of the coadsorbed oxygen to facilitate hydrogen abstraction from the nitrogen-containing surface species. It is worth noticing that ammonia decomposition on clean Ni(110) is quite limited, amounting to significantly less than the approximately 80% of the total of the ammonia monolayer seen here.[39] Above 300 K, most of the NH_x moieties dehydrogenate completely to atomic nitrogen (which recombines and desorbs around 800 K, Figure 4). An additional ~10% of the ammonia does desorb from the surface above 300 K, mostly in the recombinative 400 K state seen in the NH_3 TPD traces in Figure 1.

Finally, the main observation from the O 1s XPS yield curves in Figure 6 is the significant decrease in signal between 200 and 300 K for the atomic oxygen species, as mentioned above. This roughly corresponds to the water desorption seen in the middle panel of Figure 1. On the other hand, not much change is seen in the concentration of the surface OH groups as a function of annealing temperature. This suggests that hydroxyl formation via hydrogen extraction from the nitrogen-containing species is rate limiting and that OH groups, once formed, disproportionate rapidly to atomic oxygen and water, the latter of which desorbs from the surface. A small decrease in OH XPS signal is nevertheless seen between 250 and 300 K. The estimated coverages for the oxygen atoms that remain on the surface after the water desorption around 350 K are reported in Table 1.

3.3. Isotope Labeling Experiments. To better understand the hydrogen transfer steps involved in the reaction of ammonia coadsorbed with atomic oxygen on Ni(110) surfaces, additional TPD experiments were performed using ND_3. Unfortunately, due to the ease with which ammonia undergoes H−D exchange catalyzed by the walls of its container, it was not possible to use isotopically pure ammonia in these studies. It was determined by mass spectrometry that the commercially available fully deuterated ammonia we used had an actual composition of approximately 50% ND_3, 30% ND_2H, and 20% NDH_2. Three different sources were tried, with similar results. This complicated the interpretation of the isotope labeling TPD experiments, but did not preclude the gathering of some valuable information about the appropriate surface chemical steps. A description of the key results from these experiments is provided next.

Figure 7 displays the desorption traces for hydrogen as a function of oxygen predose. As in the case of deuterated ammonia on clean Ni(110),[39] significant deuterium desorption is observed in the 3 (HD) and 4 (D_2) amu traces, indicating appreciable decomposition of the adsorbed ammonia. Also in analogy with the case of deuterated ammonia on the clean surface, D_2 desorption is only observed above 400 K, whereas some HD production is detected in the 380 K peak. This difference in behavior between the H- and D-containing desorbing molecular hydrogen is mostly due to a kinetic isotope effect in the decomposition of adsorbed ammonia, although a small contribution from background hydrogen adsorption may play a role as well. In any case, the lack of any D_2 desorption below 400 K (and the limited production of H_2 above that temperature) indicates significant early isotope scrambling;

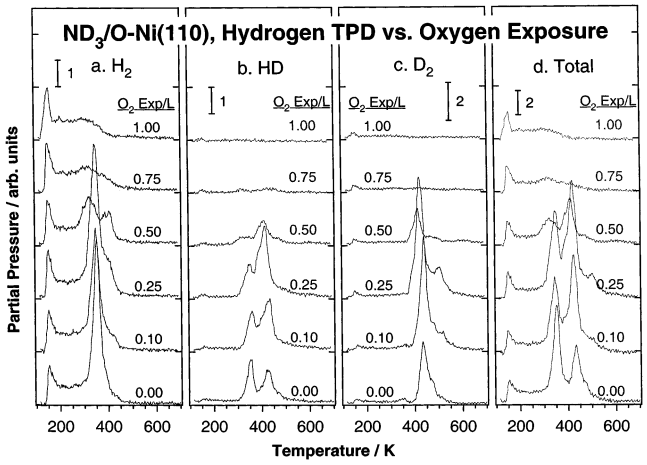

Figure 7. H_2 (2 amu, a, left), HD (3 amu, b, second from left), D_2 (4 amu, c, second from right), and total hydrogen (sum of the three sets of data, d, right) TPD traces from deuterated ammonia adsorbed on various oxygen-predosed Ni(110) surfaces. In all cases, 1.5 langmuir of ND_3 was adsorbed at 100 K after the oxygen treatments at 300 K. A clear kinetic isotope effect is manifested by the predominance of H_2 desorption below 400 K and the extensive generation of HD and D_2 above that temperature. That result also attests to extensive isotope scrambling. Significant amounts of H_2 and HD are observed because of the isotopic impurity of the deuterated ammonia (to up to a ~1:3 H:D ratio).

otherwise deuterium desorption from initial decomposition of the fully deuterated ammonia (50% of the total) should have been detected at the low temperatures where normal hydrogen is produced. Also, both an increase in the extent of the D-containing hydrogen production and the appearance of a high temperature (~500 K) peak are seen as the oxygen predose is increased to 0.25 langmuir. After that, general poisoning of the activity of the surface becomes evident. The total production of hydrogen (all isotope compositions) follows a behavior similar to that seen with NH_3 (compare Figures 1a and 7d), except that the second main feature peaks at approximately 430 K, at about 25 K higher temperature. Again, this is a clear indication of a kinetic isotope effect for the ammonia dehydrogenation steps, equivalent to an approximately 1.5 kcal/mol difference in activation energy between NH_3 and ND_3.

As stated above, the analysis of the information for molecular desorption from the experiments with deuterated ammonia is complicated by the mixed composition of the original gas. Fortunately, the isotopic composition of that gas could be determined independently by mass spectrometry (see Experimental Section). The signals for the 14−20 amu traces could then be scaled accordingly to take the composition of the original ammonia mixture into account. This is illustrated by the traces in the left panel of Figure 8, where the TPD data for a 1.5 langmuir ND_3 dose on a 0.25 langmuir O_2 predosed Ni(110) surface were scaled appropriately. In fact, because desorption from the β ammonia state does not involve any chemical reaction, all TPD signals below 250 K are expected to match those from the known ammonia gas composition and the cracking patterns of the individual ammonia isotopologues, and this was certainly the case in our experiments. Above 250 K, on the other hand, significant deviations were observed, indicative of surface isotope scrambling.

Further analysis of the TPD data from the ND_3/O/Ni(110) system was attempted by following two different procedures. The first, illustrated in the right panel of Figure 8, consisted of subtracting the TPD traces from consecutive amus. Specifically, difference spectra are shown in that figure for (20−19), (19−18), and (18−17) amu. It needs to be remembered that these data contain information about the desorption of both water and ammonia. Our second approach was to independently follow the total production of ammonia by using the signal for 14 amu, and to calculate the deviations of the signals for 17−20 amu from that desorption. Those results are provided as a function of oxygen predose in Figure 9.

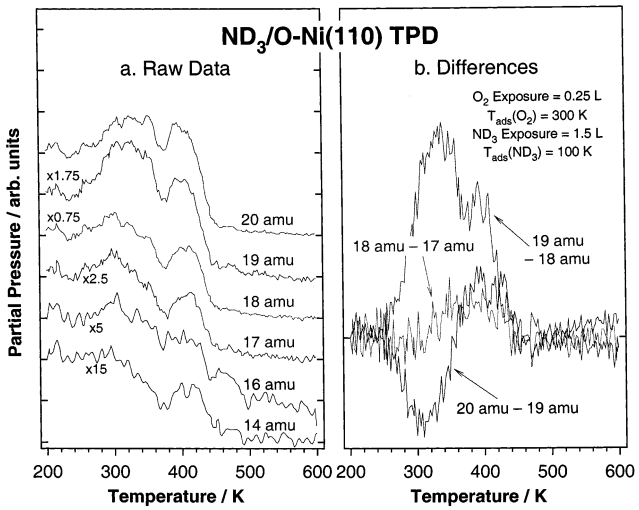

Figure 8. Left: raw 14, 16, 17, 18, 19, and 20 amu TPD data from experiments with deuterated ammonia on oxygen-pretreated Ni(110). This example corresponds to a 0.25 L O_2 predose at 300 K. The 400 K chemistry reported above is also evident in these traces, but the identification of the contributions from the different water and ammonia isotopologues to it is hampered by the extensive cracking of those species in the mass spectrometer. Right: difference spectra between consecutive masses, obtained by subtraction of the corresponding raw data reported in the left panel. The preferential production of heavy water at higher temperatures is manifested by the transition from negative to positive values seen around 360 K in the 20−19 amu trace.

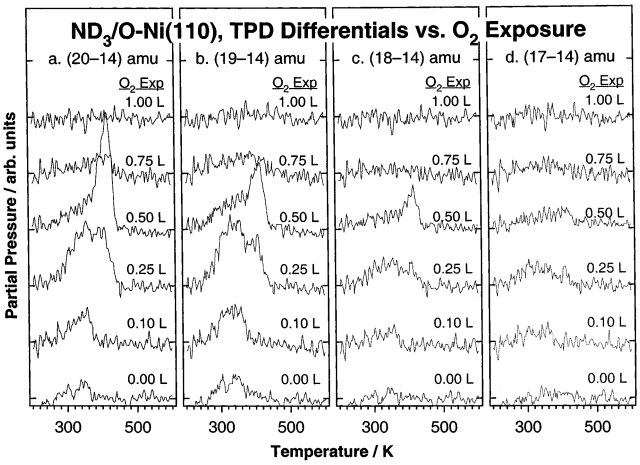

Figure 9. Difference TPD spectra for deuterated ammonia on O/Ni(110) surfaces as a function of oxygen predose. The four panels in this case correspond to the data obtained by subtracting the 14 amu TPD signal (representative of total ammonia production) from the 20 (a, left), 19 (b, second from left), 18 (c, second from right), and 17 (d, right) amu traces. The positive peaks seen in all cases indicate the predominance of contributions from water production in those signals. Also, a larger contribution is again seen at higher temperatures for the cases of the heavier water isotopologues.

There are at least two clear desorption states differentiated in Figures 8 and 9, one between 250 and 350 K, and a second around 400 K. These could be easily associated with the α and high-temperature ammonia states identified earlier with normal ammonia, respectively. The data indicate that there is a clear

difference in the behavior of the different traces in the first temperature range. However, although some isotope scrambling within the adsorbed ammonia can be seen above 250 K even on clean nickel,[39] most of the features observed in Figures 8 and 9 shown here can be ascribed to water formation. For one, only positive deviations from the 14 amu signal are seen for the 17 to 20 amu range (Figure 9). This is in contrast with the decrease in population of the α-NH_3 state observed in Figure 1b as the oxygen predose was increased from 0 to 0.60 langmuir. In addition, most of the behavior seen in Figure 9 resembles that seen for water desorption in Figure 1c. Indeed, there is first a growth in the water 350 K peak, up to a 0.10 langmuir O_2 predose, then the appearance of a second feature about 415 K between 0.25 and 0.50 langmuir O_2, and finally the suppression of most of the water production above 0.75 langmuir O_2.

Note also that, once again, there are noticeable kinetic isotope effects associated with the production of water. Specifically, the isotopic composition of the desorbing water changes with temperature, hence the structures seen in the difference spectra reported in Figure 8b. For instance, the negative peak around 310 K and the positive incursion around 380 K in the (20−19) amu trace provides a clear indication that lighter (HDO, the 19 amu signal) water is formed at lower temperatures relative to D_2O (the 20 amu component). In addition, both Figures 8 and 9 show that the high-temperature water peak shifts with deuterium substitution, from 405 K for H_2O to 415 K for D_2O. Finally, the relative yields for D_2O and HDO in the 415 K feature are higher relative to those around 350 K. For instance, the (17−14) and (18−14) amu traces for the 0.25 langmuir O_2 predose in Figure 9 show water desorption mostly from the 350 K state, whereas those for (19−14) and (20−14) amu have significant contributions about 410 K. Similar arguments can be made for the traces for the 0.50 langmuir O_2 predose.

4. Discussion

The TPD and XPS data reported here help further advance our understanding of the chemistry of ammonia with atomic oxygen on Ni(110), and more generally of the acid−base chemistry of similar systems. The NH_3/O/Ni(110) case has been investigated before,[3,23,25,42,52] but no systematic study on the interaction of the coadsorbates as a function of surface coverages has been reported to date, and only limited discussion has been advanced on the thermal chemistry of ammonia on the oxygen-treated nickel surfaces. Our TPD data as a function of oxygen and ammonia exposures, the associated XPS information, and the isotope labeling experiments, all point to a clear picture of the surface chemistry between the two reactants based on hydrogen-transfer steps between adjacent O(ads) and NH_x(ads) species.

The first thing to notice from the NH_3 TPD traces in Figure 1b is that there is an initial drop in total ammonia molecular desorption with increasing oxygen coverage on the surface. Most of that reduction, seen between 0 and 0.50 langmuir O_2 predoses, takes place in the so-called α-NH_3 state, between 250 and 350 K. Because that state is associated with direct adsorption on the nickel surface, it could be easily argued that the drop in ammonia yield is a direct result from site blocking by oxygen atoms. However, oxygen adsorption is known to induce a series of surface reconstructions on Ni(110), creating new −Ni−O− chains in the [001] direction that help bring additional nickel atoms to the surface.[28] In fact, after reaching a minimum at an oxygen predose of about 0.50 langmuir, the yield for molecular ammonia desorption increases again at higher oxygen coverages. Instead, most of the NH_3 yield drop at intermediate oxygen coverages can be accounted for by an increase in ammonia decomposition. Note that, indeed, the ∼0.1 monolayer dip seen for ammonia molecular desorption in Figure 2b is matched by the corresponding increase in nitrogen desorption (from ammonia decomposition) reported in Figure 4. There is also a dip in the initial ammonia sticking coefficient within the same oxygen predose range (Figure 3), indicating that changes in the electronic structure of the surface may play a role as well.

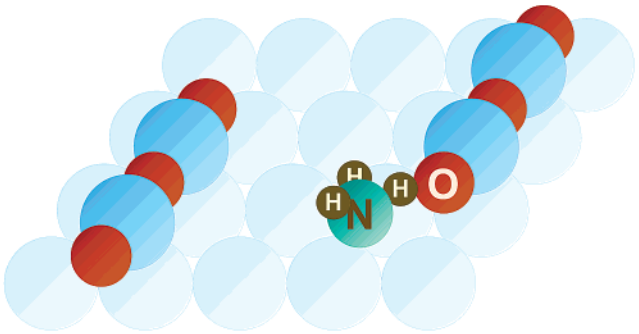

Figure 10. Schematic representation of the proposed surface arrangement of the oxygen and ammonia reactants responsible for the chemistry that takes place around 400 K in the NH_3/O/Ni(110) system. It is suggested that the oxygens at the end of the [001]-oriented −Ni−O− rows produced by the oxygen-induced reconstruction of the Ni(110) surface are particularly reactive, and interact via hydrogen-bonding with ammonia molecules bonded to adjacent nickel atoms. The hydrogen transfer is reversible, hence the extensive isotope scrambling in the experiments with ND_3, but it favors water formation, presumably because of the higher electronegativity of oxygen compared to that of nitrogen.

Perhaps the most significant observation from the TPD data for ammonia on oxygen-predosed Ni(110) is the appearance of a new reaction channel around 400 K at intermediate oxygen coverages. This new state was first observed by Madey and Benndorf,[23] who also reported the formation of "tilted" OH groups on the surface starting at 200 K. Bassignana et al. advanced the idea that the observed increase in ammonia decomposition may be due to an increase in binding energy for ammonia in the presence of coadsorbed oxygen,[42] but Ruan and co-workers argued that such an explanation does not account for the maximum in reactivity at oxygen coverages of only 0.1−0.2 monolayer.[52] Instead, they proposed that the key lies in the possibility of a direct interaction between the NH_3 molecules and the terminating oxygen atoms in the short, mobile, −Ni−O− added rows that form on the surface under these conditions. We agree with this latter interpretation, and add that the fundamental interaction responsible for the activation of the adsorbed ammonia is a hydrogen bond to an adjacent oxygen surface atom. The proposed model is depicted schematically in Figure 10.

Several pieces of evidence can be invoked to support the hydrogen-bonding mechanism discussed above. Perhaps the most convincing is the one already mentioned before, namely, the fact that the yields for the high-temperature (∼400 K) chemistry observed in the TPD experiments is maximized at the intermediate oxygen coverages where large concentrations of end-row oxygen atoms are expected on the reconstructed surface. This strongly suggests that a direct side-by-side interaction is required between the oxygen atoms and ammonia molecules bonded to the nickel surface atoms. Note that, in ammonia uptake experiments such as those in Figure 3, the chemistry at ∼400 K is the one that manifests itself first in the TPD data. In addition, the XPS data in Figure 5 point to the formation of partially hydrogenated oxygen- (OH) and nitrogen-containing (NH, NH_2) molecules. The detection of large amounts

of NH and NH_2 surface moieties around 300 K (Figure 6) suggests that those are involved in the hydrogenation−dehydrogenation steps observed above that temperature. Finally, the isotope scrambling observed in the TPD data in Figures 8 and 9 points to hydrogen transfer from the adsorbed ammonia to the coadsorbed oxygen atoms. Of particular importance here is the fact that most of the deuterium atoms in the deuterated ammonia end up in the water that desorbs above 300 K. Because no water formation is observed after exposing oxygen-predosed Ni(110) surfaces to molecular hydrogen or deuterium (data not shown), it can be concluded that hydrogen transfer most likely occurs directly via H-bonding.

Two additional points can be made on the high-temperature chemistry of ammonia with atomic oxygen on Ni(110). First, the hydrogen transfers between the two surface species must take place in a stepwise fashion (one at a time), because (1) both NH and NH_2 species have been proposed to form on the surface, (2) the 400 K ammonia TPD peak is most likely associated with the rehydrogenation of adsorbed NH_2 fragments, and (3) all the isotopolgues of water (H_2O, HDO, D_2O) can be detected in TPD experiments with ND_3. Second, it is quite likely that most of this chemistry takes place directly between the two reactants (adsorbed next to each other), and not via hydrogen transfer through the nickel surface, because almost no water or high-temperature ammonia is seen in experiments with oxygen or ammonia coadsorbed with atomic hydrogen (data not shown). Dehydrogenation of hydrogen-containing species (ammonia) at high temperatures may nevertheless be required to provide the required hydrogen atoms for water and ammonia production above 380 K, which otherwise would recombine and desorb as H_2 at much lower temperatures. That proviso aside, we advance the notion that the 400 K chemistry seen between ammonia and oxygen coadsorbed on Ni(110) surfaces takes place via reversible interconversion along the following reaction pathway:

$$NH_3(ads) + O(ads) \leftrightarrow NH_2(ads) + OH(ads) \leftrightarrow NH(ads) + H_2O(ads) \quad (1)$$

The extent of the reversibility of this sequence of reactions in the high-temperature (∼400 K) regime will be addressed next. One simplified way of probing the relative probabilities for the forward and backward steps in this mechanism is to explore the possible equilibria among the nitrogen- and oxygen-containing species. In that respect, the reaction scheme proposed in eq 1 should eventually lead to the overall conversion:

$$2NH_3 + 3O(ads) = 3H_2O + 2N(ads) \quad (2)$$

It is clear that, in this reaction, the formation of water is favored. The following pieces of evidence can be offered in support of this conclusion: (1) the production of water peaks at an earlier (395 K) temperature than the desorption of ammonia (400 K); (2) the total amount of water produced in this state is up to 5 times larger than that of ammonia; (3) the maximum in 395 K water production is achieved at oxygen precoverages slightly higher than those needed for the optimum production of the 400 K ammonia (0.6 vs 0.3 langmuir)—an indication that the oxygen coverage drives eq 2 to the right; and (4) a significant amount of the deuterium atoms in the experiments with ND_3 end up in the desorbing water.

Significant amounts of ammonia are eventually converted to water, but that process does not reach equilibrium under the conditions of our experiments. Proof of this comes from our calculations of the reaction quotients $Q(2)$ for eq 2 provided in Table 1. There, the surface concentrations of nitrogen and oxygen just before the onset of the ∼400 K state are combined with the corresponding H_2, NH_3, and H_2O TPD high-temperature yields in the TPD experiments to estimate the ratios associated with three different equilibria. It can be seen that the $Q(2)$ value varies systematically with increasing oxygen predose, a clear indication that the measured surface concentrations do not represent their equilibrium values. On the other hand, the fractions of the NH_x fragments that rehydrogenate back to ammonia or decompose all the way to nitrogen do vary with Θ_O as well, indicating that the kinetics of those steps are not simple but involve some degree of reversibility and competition with other parallel reactions. In fact, a significant fraction of the ammonia that remains on the surface above 370 K ends up dehydrogenating all the way to atomic nitrogen, although that fraction decreases monotonically with increasing oxygen precoverage, from over 95% after a 0.025 langmuir O_2 predose to less than 20% for the 1.0 langmuir O_2 case. Total ammonia dehydrogenation can be summarized by the overall reaction:

$$2NH_3 = 2N(ads) + 3H_2 \quad (3)$$

As can be seen in Table 1, eq 3 is also not in equilibrium: no constant value of $Q(3)$ associated with $K_{eq}(3)$ is obtained with varying oxygen predose.

Finally, water formation via hydrogen transfer from ammonia, eq 1, competes with the recombination of surface hydroxyl groups:

$$2OH(ads) = H_2O + O(ads) \quad (4)$$

This latter reaction is known to occur on Ni(110),[43,44] as well as other,[1,53] surfaces dosed with oxygen and water, and to yield a similar high-temperature water TPD peak as the one reported here with coadsorbed ammonia. The concentration of OH groups in our ammonia + oxygen experiments was always low (Figures 5 and 6), suggesting that those species are transient, and that they disproportionate according to eq 4 as soon as they are formed (via hydrogen transfer from NH_x species). Nevertheless, the importance of this channel can be probed by investigating the overall equilibrium:

$$H_2 + O(ads) = H_2O \quad (5)$$

The data in Table 1 shows that an approximately constant value of $Q(5) = 9 \pm 2$ monolayers^{-1} is obtained, suggesting that water formation (as opposed to ammonia hydrogenation−dehydrogenation) is rapid and reversible, that is, that $K_{eq}(5)$ can indeed be equated to the average $Q(5)$ value. The extensive isotope scrambling seen in the desorbing water in Figure 9 corroborates this conclusion.

The picture that emerges is one where nitrogen- and oxygen-containing adsorbates behave in a qualitatively similar fashion. It is clear that the reversible hydrogen transfer among adjacent O(ads), OH(ads), H_2O(ads), N(ads), NH(ads), NH_2(ads), and NH_3(ads) surface species is facilitated by the initial formation of hydrogen bonds. It is also evident that the oxygen-containing species are more stable than their nitrogen counterparts. Therefore, the conversion in systems with coadsorbed oxygen and ammonia shifts toward the formation of water. This is what is expected from basic acid−base chemistry: given that oxygen is more electronegative than nitrogen, both O and OH species are expected to act as bases in the presence of more acidic nitrogen-containing moieties, and to therefore induce the abstraction of hydrogen atoms from those. It appears that the nickel surface does not significantly alter this trend.

It should be noted that the reactivity of ammonia coadsorbed with oxygen reported here may very well be quite general. Indeed, some aspects of this chemistry have already been reported for other surfaces. For instance, the assistance of coadsorbed oxygen in dissociating ammonia has been reported on Ag(110).[54] STM work led to a proposal of reactivity involving the [001] oriented −Ag−O− rows that form on that surface, the same as on nickel.[27] Similar chemistry has been reported on Cu(110).[26,55] In more general terms, partially oxygen-covered metal surfaces have shown unique chemistry not seen either on the clean surface or on a fully oxidized substrate. One example of this is provided by our studies of the partial oxidation of alkyls and alcohols on O/Ni(100).[10,11,20,21,56] It was found that 2-propyl moieties can be converted to acetone through a two-step mechanism involving the facile incorporation of oxygen atoms to form 2-propoxide groups[56] and the subsequent β-hydride elimination from those intermediates to acetone.[10] In analogy with the ammonia + oxygen system, that reaction only takes place at submonolayer oxygen coverages, perhaps with particularly reactive oxygen atoms such as those at the end of the Ni−O− chains in Ni(110), and involves adjacent alkyl and oxygen groups.

Finally, the results from the ammonia titration studies reported here can be used to understand more complex and realistic catalytic systems. In particular, the reactive oxygen atoms identified in this study can very well represent specific sites in defective nickel oxide catalysts. It is worth pointing out that such sites can indeed be produced by sputtering of stoichiometric NiO films.[36] Selective alcohol dehydrogenation has also been seen on nickel foils and on supported nickel catalysts with thin partially oxidized surfaces.[11,21,57,58] An active form of oxygen, different from the lattice O atoms in NiO, was identified as the reactive species in those studies.[59,60] The acidic character and lability of the end-of-chain oxygen atoms reported here is consistent with such observations.

5. Conclusions

The chemistry of ammonia with coadsorbed oxygen on Ni(110) surfaces was characterized by temperature-programmed desorption (TPD) and X-ray photoelectron spectroscopy (XPS). The preadsorption of oxygen on the surface modifies the behavior of adsorbed ammonia in two fundamental ways: (1) it blocks sites for the direct bonding of ammonia to nickel atoms, thus suppressing the population of the so-called α-NH_3 state, the one that desorbs molecularly between 250 and 350 K, and (2) it induces new chemistry around 400 K. The latter is manifested by new TPD features for water and ammonia around 395 and 400 K, respectively, and by a significant increase in the desorption of molecular hydrogen at 405 K. The yields for this state reach maxima at intermediate oxygen coverages, that is, after an oxygen predose of about 0.3 langmuir, which corresponds to a surface coverage of atomic oxygen of about 0.14 monolayer, and decrease again at higher Θ_O. The reactivity seen about 400 K is associated with hydrogen transfer between the coadsorbed ammonia and atomic oxygen, as manifested by the following observations: (1) there is an increase in the decomposition of ammonia, as seen by the subsequent desorption of molecular nitrogen around 800 K; (2) the formation of NH_2 and NH species on the surface is indicated by the appearance of a new N 1s XPS feature about 397.2 eV, the maximum intensity of which is attained around 300 K; and (3) significant isotope scrambling is observed in TPD experiments with ND_3, where significant amounts of deuterated water are produced. This hydrogen transfer is proposed to take place via hydrogen bonding with oxygen atoms at the end of the reconstructed −Ni−O− rows that form on Ni(110) at intermediate oxygen coverages. Finally, the interconversion of ammonia + oxygen to water + nitrogen is biased toward the latter mix, as suggested by the following observations in the 400 K surface chemistry: (1) the lower temperature of the water peak (395 K) compared to ammonia feature (400 K) in the TPD experiments; (2) the larger H_2O yields, often over 5 times those for ammonia; (3) the earlier formation of water than ammonia as a function of initial NH_3 dose in uptake experiments with preset oxygen predoses; (4) the significant scrambling of normal hydrogen and deuterium in the water produced with ND_3; and (5) the fact that the formation of water from adsorbed oxygen and hydrogen appears to reach an equilibrium under the conditions of the TPD experiments. All these observations are believed to be quite general, extending to other metals, and to reflect the fundamental acid−base surface chemistry of oxide surfaces.

Acknowledgment. Financial support for this research was provided by the Department of Energy, Basic Energy Sciences Division, under contract DE-FG03-01ER15182.

References and Notes

(1) Thiel, P. A.; Madey, T. E. *Surf. Sci. Rep.* **1987**, *7*, 211.
(2) Huntley, D. R. *Surf. Sci.* **1990**, *240*, 24.
(3) Kulkarni, G. U.; Rao, C. N. R.; Roberts, M. W. *J. Phys. Chem.* **1995**, *99*, 3310.
(4) Surman, M.; Lackey, D.; King, D. A. *J. Electron Spectrosc. Relat. Phenom.* **1986**, *39*, 245.
(5) Roberts, J. T.; Madix, R. J. *Surf. Sci.* **1990**, *226*, L71.
(6) Ayre, C. R.; Madix, R. J. *J. Am. Chem. Soc.* **1995**, *117*, 2301.
(7) Jones, G. S.; Barteau, M. A.; Vohs, J. M. *J. Phys. Chem. B* **1999**, *103*, 1144.
(8) Solymosi, F. *J. Mol. Catal. A* **1998**, *131*, 121.
(9) Queeney, K. T.; Friend, C. M. *J. Phys. Chem. B* **2000**, *104*, 409.
(10) Gleason, N. R.; Zaera, F. *J. Catal.* **1997**, *169*, 365.
(11) Zaera, F.; Gleason, N. R.; Klingenberg, B.; Ali, A. H. *J. Mol. Catal. A* **1999**, *146*, 13.
(12) Bielanski, A.; Haber, J. *Oxygen in Catalysis*; Marcel Dekker: New York, 1991.
(13) Endo, M.; Matsumoto, T.; Kubota, J.; Domen, K.; Hirose, C. *Surf. Sci.* **1999**, *441*, L931.
(14) Weng, W.; Chen, M.; Wan, H.; Liao, Y. *Catal. Lett.* **1998**, *53*, 43.
(15) Li, W.; Gibbs, G. V.; Oyama, S. T. *J. Am. Chem. Soc.* **1998**, *120*, 9041.
(16) Burrington, J. D.; Grasselli, R. K. *J. Catal.* **1979**, *59*, 79.
(17) Gamble, L.; Jung, L. S.; Campbell, C. T. *Surf. Sci.* **1996**, *348*, 1.
(18) Lusvardi, V. S.; Barteau, M. A.; Dolinger, W. R.; Farneth, W. E. *J. Phys. Chem.* **1996**, *100*, 18183.
(19) Rekoske, J. E.; Barteau, M. A. *J. Catal.* **1997**, *165*, 57.
(20) Gleason, N. R.; Zaera, F. In *3rd World Congress on Oxidation Catalysis, San Diego, California, 21−26 September 1997 (Studies in Surface Science and Catalysis Series, Vol. 110)*; Grasselli, R. K., Oyama, S. T., Gaffney, A. M., Lyons, J. E., Eds.; Elsevier: Amsterdam, 1997; p 235.
(21) Zaera, F. *Catal. Today*, in press.
(22) Seabury, C. W.; Rhodin, T. N.; Purtell, R. J.; Merrill, R. P. *Surf. Sci.* **1980**, *93*, 117.
(23) Madey, T. E.; Benndorf, C. *Surf. Sci.* **1985**, *152−153*, 587.
(24) Wu, M.-C.; Truong, C. M.; Goodman, D. W. *J. Phys. Chem.* **1993**, *97*, 4182.
(25) Dastoor, H. E.; Gardner, P.; King, D. A. *Surf. Sci.* **1993**, *289*, 279.
(26) Guo, X.-C.; Madix, R. J. *J. Chem. Soc., Faraday Trans.* **1997**, *93*, 4197.
(27) Guo, X. C.; Madix, R. J. *Surf. Sci.* **2002**, *501*, 37.
(28) Eierdal, L.; Besenbacher, F.; Laegsgaard, E.; Stensgaards, I. *Surf. Sci.* **1994**, *312*, 31.
(29) Freund, H. J.; Dillmann, B.; Seiferth, O.; Klivenyi, G.; Bender, M.; Ehrlich, D.; Hemmerich, I.; Cappus, D. *Catal. Today* **1996**, *32*, 1.
(30) Pai, W. W.; Reutt-Robey, J. E. *Phys. Rev. B* **1996**, *53*, 15997.
(31) Coulman, D. J.; Wintterlin, J.; Behm, R. J.; Ertl, G. *Phys. Rev. Lett.* **1990**, *64*, 1761.
(32) Ertl, G. *Catal. Rev.−Sci. Eng.* **1980**, *21*, 201.

(33) Grunze, M. In *The Chemical Physics of Solid Surfaces and Heterogeneous Catalysis*; King, D. A., Woodruff, D. P., Eds.; Elsevier: Amsterdam, 1982; Vol. 4 (Fundamental Studies of Heterogeneous Catalysis), p 143.
(34) Grasselli, R. K. In *Handbook of Heterogeneous Catalysis*; Ertl, G., Knözinger, H., Weitkamp, J., Eds.; VCH: Weinheim, 1997; Vol. 5, p 2302.
(35) Guo, H.; Zaera, F. *Surf. Sci.*, in press.
(36) Öfner, H.; Zaera, F. *J. Phys. Chem. B* **1997**, *101*, 9069.
(37) Chrysostomou, D.; Zaera, F. *J. Phys. Chem. B* **2001**, *105*, 1003.
(38) Klauber, C.; Alvey, M. D.; Yates, J. T., Jr. *Surf. Sci.* **1985**, *154*, 139.
(39) Chrysostomou, D.; Flowers, J.; Zaera, F. *Surf. Sci.* **1999**, *439*, 34.
(40) Holloway, P. H.; Hudson, J. B. *Surf. Sci.* **1974**, *43*, 123.
(41) Brundle, C. R. In *The Chemical Physics of Solid Surfaces and Heterogeneous Catalysis*; King, D. A., Woodruff, D. P., Eds.; Elsevier: Amsterdam, 1990; Vol. 3A (Chemisorption Systems), p 132.
(42) Bassignana, I. C.; Wagemann, K.; Küppers, J.; Ertl, G. *Surf. Sci.* **1986**, *175*, 22.
(43) Callen, B. W.; Griffiths, K.; Memmert, U.; Harrington, D. A.; Bushby, S. J.; Norton, P. R. *Surf. Sci.* **1990**, *230*, 159.
(44) Guo, H.; Zaera, F. Manuscript to be published.
(45) de Jesús, J. C.; Carrazza, J.; Pereira, P.; Zaera, F. *Surf. Sci.* **1998**, *397*, 34.
(46) Grunze, M.; Dowben, P. A.; Brundle, C. R. *Surf. Sci.* **1983**, *128*, 311.
(47) Kim, K. S.; Winograd, N. *Surf. Sci.* **1974**, *43*, 625.
(48) de Jesús, J. C.; Pereira, P.; Carrazza, J.; Zaera, F. *Surf. Sci.* **1996**, *369*, 217.
(49) McIntyre, N. S.; Cook, M. G. *Anal. Chem.* **1975**, *47*, 2208.
(50) Uhlenbrock, S.; Scharfschwerdt, C.; Neumann, M.; Illing, G.; Freund, H.-J. *J. Phys. Condens. Matter* **1992**, *4*, 7973.
(51) de Jesús, J. C.; Gleason, N.; Zaera, F. In *211th American Chemical Society National Meeting*; New Orleans, 1996; Paper No. COLL-143.
(52) Ruan, L.; Stensgaard, I.; Lægsgaard, E.; Besenbacher, F. *Surf. Sci.* **1994**, *314*, L873.
(53) Heras, J. M.; Viscido, L. *Catal. Rev.—Sci. Eng.* **1988**, *30*, 281.
(54) Thornburg, D. M.; Madix, R. J. *Surf. Sci.* **1989**, *220*, 268.
(55) Afsin, B.; Davies, P. R.; Pashusky, A.; Roberts, M. W.; Vincent, D. *Surf. Sci.* **1993**, *284*, 109.
(56) Zaera, F.; Guevremont, J. M.; Gleason, N. R. *J. Phys. Chem. B* **2001**, *105*, 2257.
(57) Ali, A. H.; Zaera, F. *J. Mol. Catal. A* **2002**, *177*, 215.
(58) Zaera, F. *Int. Rev. Phys. Chem.* **2002**, *21*, 433.
(59) Ali, A. H. Ph.D. Thesis Thesis, University of California, Riverside, 2002.
(60) Ali, A. H.; Zaera, F. Mansucript to be published.